Environmental Science and Pollution Research (2019) 26:3330–3339
https://doi.org/10.1007/s11356-018-3868-z

RESEARCH ARTICLE

Adsorptive removal of lead from acid mine drainage using cobalt-methylimidazolate framework as an adsorbent: kinetics, isotherm, and regeneration

Azile Nqombolo[1,2] · Anele Mpupa[1] · Aphiwe S. Gugushe[1] · Richard M. Moutloali[1,2] · Philiswa N. Nomngongo[1,2]

Received: 28 August 2018 / Accepted: 27 November 2018 / Published online: 3 December 2018

Abstract

In this work, cobalt-methylimidazolate framework has been used as an adsorbent in the removal of Pb(II) from acid mine drainage in adsorption batch system. X-ray diffraction, Fourier-transform infrared spectroscopy, Brunauer-Emmet-Teller and transmission electron microscope were used for structural, morphological, and surface characteristics of cobalt-methylimidazolate framework. The concentration of heavy metal ions in water samples was measured by inductively coupled plasma optical emission spectrometry. Different experimental factors/variables (such as contact time, dosage, and pH) affecting the adsorption of Pb(II) from acid mine drainage were optimized by response surface methodology based on central composite design. Under optimized experimental parameters, the maximum adsorption capacity of Pb(II) was found to be 105 mg g^{-1}. The nature of the adsorption process was investigated using Langmuir and Freundlich isotherm models. The obtained data best fitted Langmuir isotherm model suggesting a homogeneous adsorption process. Furthermore, the adsorption mechanism was investigated using five kinetic models, that is, pseudo-first order, pseudo-second order, intraparticle diffusion and Elovich model. The adsorption data fitted better to pseudo-second-order followed by intra-particle diffusion kinetic models suggesting that the adsorption mechanism is dominated by both chemical and physical adsorption processes. The adsorbent could be regenerated up to 8 cycles and it was successfully used in the removal of lead in real acid mine drainage samples.

Keywords Heavy metals · Zeolitic imidazolate framework · Lead · Wastewater · Acid mine drainage · Adsorption

Introduction

Population growth poses high demand on clean water supply, as water quality is most important for human consumption and agricultural purposes (Kummu et al. 2016; Sahin et al. 2015). Various means of producing clean water by treating wastewater have been reported in literature but the main issue is the presence of pollutants such as heavy metals in water which turns to threaten human health and aquatic life (Sadegh et al. 2017). Water contamination by heavy metals such as Cd, Pb, As, and Hg is one of the main environmental problems. This is because these metals are found to be toxic even at very low concentrations (Le Pape et al. 2017). The presence of toxic soluble contaminants in water is of great concern. For this reason, several researchers have developed different strategies to remove these contaminants especially toxic trace metals (Fernandez-Rojo et al. 2017; Premkumar et al. 2018; Maarof et al. 2017). These methodologies include coagulation (Marzougui et al. 2017), membrane filtration (Yurekli 2016) and adsorption (Lee et al. 2015; Ungureanu et al. 2015). Among the abovementioned methods, adsorption technology is the preferred method due to its low cost, flexibility, simplicity, and effectiveness in removing heavy metals and has been applied in different

Responsible editor: Tito Roberto Cadaval Jr

Electronic supplementary material The online version of this article (https://doi.org/10.1007/s11356-018-3868-z) contains supplementary material, which is available to authorized users.

✉ Philiswa N. Nomngongo
pnnomngongo@uj.ac.za; nomngongo@yahoo.com

[1] Department of Applied Chemistry, University of Johannesburg, Doornfontein Campus, P.O. Box 17011, Johannesburg 2028, South Africa

[2] DST/Mintek Nanotechnology Innovation Centre, Water Research Node P.O. Box 17011, Doornfontein, Johannesburg 2028, South Africa

industries (Perrich 2018; Xu and McKay 2017; Al-Qodah et al. 2017). In addition, an attractive feature of adsorption method is the use of different adsorbents.

Researches have used different porous adsorbents to remove pollutants from wastewater and other complex matrices. The choice of these adsorbents is due to their porosity and large surface area. These adsorbents include activated carbon (Dimpe et al. 2017), mesoporous carbon (Aldawsari et al. 2017; Nayak et al. 2017), nanometal oxides (Santhosh et al. 2017; Dey 2012), carbon nanotubes (Yadav and Srivastava 2017), metal organic frameworks (MOFs) (Huang et al. 2018a, b), and zeolites (Zanin et al. 2017). Metal organic frameworks are designed by self-assembly of the metal ion and coordinating ligands which help increase porosity of the MOF (Jin et al. 2017). These materials have been used in different applications owing to their tuneable pore size and shape (Kang et al. 2017). Most of well-studied MOFs are not water stable; therefore, in order to get water stable MOFs, hydrophilic groups are incorporated near coordination sites as this helps in hydrolysis to protect coordination bonds, and use metals with high oxidation states (such as Zr^{4+}, Fe^{3+}, Cr^{3+} and Al^{3+}) in order to coordinate strongly with organic linkers (Huang et al. 2017). Zeolitic imidazolate frameworks (ZIFs), sub-class of MOFs, are water stable. These materials pose superior and specific functional groups which increase porosity and help in increasing adsorption capacity (Li et al. 2017). ZIFs have gained much attention due to their porosity, higher chemical stability as well as positive charge, and they have been used in different applications—adsorption (Jung et al. 2015), gas separation (Wu et al. 2018), gas storage (Panchariya et al. 2018), among others (Gomar and Yeganegi 2018; Han et al. 2018). These porous materials have been used in adsorption of hazardous organic compounds such as pesticides (Zhang et al. 2017), dyes (Samal et al. 2018), personal care products/ pharmaceuticals (An et al. 2018), and heavy metals (Huang et al. 2018a, b; Bo et al. 2018; Huo et al. 2018).

In adsorption process, traditional technique of optimizing one factor at a time (OFAT) in order to determine the variable response effect, is unrealistic as it does not signify interacting effect between various factors (Mohajeri et al. 2010). For this reason, statistical design of experiments is one suitable method for obtaining useful and statistically significant models (Saeed et al. 2015). This method allows a smallest number of calculated experiments to be carried out and it considers interactions among the factors (Saeed et al. 2015). Response surface methodology (RSM) is a statistical experimental method use to find the optimum conditions for a multivariable system. This approach originates from experimental methodology which has interactive effects among other parameters that influence the analytical response (Amini et al. 2008).

Herein, we report adsorptive removal of Pb(II) using cobalt-methylimidazolate framework (ZIF-67) as an adsorbent in adsorption of Pb(II) from acid mine drainage (AMD). According to the literature search, there are few recent reports on the use of ZIF-67 in removal of Cr(VI) (Shahrak et al. 2017), Pb, and Cu (Huang et al. 2018a, b). RSM based on central composite design (CCD) was used to optimize the interactive effects of sample pH, mass of adsorbent, and contact time.

Experimental

Materials and reagents

All solvents and reagents were commercially obtainable, and they were used as received. Ammonium solution, methanol, polyvinylpyrrolidone (PVP), acetic acid, 0.22-μm PVDF syringe filters, lead standard (10,000 mg L^{-1}), 2-methylamidazole, and cobalt(II) nitrate hexahydrate were obtained from Sigma-Aldrich (St. Loius, MO, USA). Working standards of lead were prepared daily by diluting the amount of lead stock solution.

Instrumentation

The oven (Xi'an Unique Electronics, UQ 9053A, Shaanxi, China) was mostly used for drying of materials. Fourier-transform infrared spectroscopy (ATR-FTIR) spectrum of the adsorbent was obtained using a Perkin Elmer Spectrum 100 FTIR spectrometer (Waltham, MA, USA) between the scan ranges of 400–4000 cm^{-1} at a resolution of 4 cm^{-1}. The morphological properties of the adsorbent were studied using transmission electron microscope (TEM JOEL JEM-2100, Japan). The crystalline structure of ZIF-67 was determined using X-ray diffraction (XRD). The surface area of the adsorbent was obtained from Brunauer-Emmett-and-Teller (BET) multipoint method by means of surface area and porosity analyzer (ASAP2020 V3. 00H, Micromeritics Instrument Corporation, Norcross, USA) using nitrogen gas, and the sample was degassed for 10 h at 110 °C. The gas used for analysis (ICP-OES) was of instrument grade. For the determination of lead ions from synthetic and real samples, inductively coupled plasma optical emission spectrometry (ICP-OES, iCAP 6500 Duo, Thermo Scientific, UK) equipped with a charge injection device detector. For adsorption studies, a Branson 5800 ultrasonic cleaner (Danbury, CT, USA) was used. The pH of both synthetic and real samples was measured by pH meter (Mettler-Toledo FE20, Switzerland). Eppendorf 5702 centrifuge (Eppendorf Ag, Hamburg, Germany) was used to separate the adsorbent form sample solutions.

Table 1 Experimental levels and range of independent variables

Parameters	Lower level (−)	Central point (0)	Higher level (+)
Adsorbent dosage (mg)	10	20	30
Contact Time (min)	5	19.5	34
pH	3.2	6.5	9.7

Synthesis of ZIF-67

ZIF-67 was prepared according to Zhang et al. (2016). Briefly, 2.08 g of 2-methylimidazole was dissolved in 40 mL of methanol, on the other hand, 520 mg of $Co(NO_3)_2{\cdot}6H_2O$ and 600 mg of PVP were dissolved in 30 mL of methanol and 10 mL of deionized water respectively. Both solutions were combined and stirred 24 h at room temperature, the product obtained was centrifuged, washed with ethanol three times then dried at 60 °C for 10 h (Zhang et al. 2016).

Adsorption procedure

The stock solution of lead (1000 mg L^{-1}) was prepared from 10,000 mg L^{-1} lead standard and diluted to the required concentrations (1–10 mg L^{-1}). The experiments were done at 25 °C in batch mode. The pH of the solutions was adjusted to the required values (3.2–9.7) by adding either 1 mol L^{-1} of acetic acid or 1 mol L^{-1} of ammonium solution. Appropriate amounts of an adsorbent (10–30 mg) were placed in precleaned polypropylene sample bottles followed by addition of synthetic sample (15 mL) containing Pb(II) with concentrations varying from 1 to 10 mg L^{-1}. The mixture was sonicated for 5–33 min. The mixture was centrifuged then filtered by means of a syringe fitted with a 0.22-μm PVDF filter to separate the supernatant from the adsorbent. The initial as well as equilibrium concentrations of Pb(II) were measured by ICP-OES. The removal efficiency of the adsorbent was then calculated using (Eq. 1):

$$\%RE = \frac{C_0 - C_e}{C_0} \times 100 \quad (1)$$

Where C_0: initial and C_e:equilibrium concentrations after adsorption.

The adsorption capacity (q_e) was calculated using (Eq. 2):

$$q_e = \frac{(C_0 - C_i)V}{M} \quad (2)$$

Where M: mass of the adsorbent used (g) and V: volume synthetic sample (L).

Factors affecting the adsorption process were determined using RSM based on central composite design (CCD). The design matrix was computed using the values (minimum, central point, and maximum) tabulated in Table 1. The experimental data was analyzed using Statistic software (version 13).

Results and discussion

Characterization

The crystalline structure of ZIF-67 was examined by X-ray diffraction (XRD) measurements (Fig. 1). Literature reported that the XRD pattern of ZIF-67 could be indexed as: 7.3° (011), 10.3° (002), 13.7° (022), 17.9° (013), 18.3° (222),

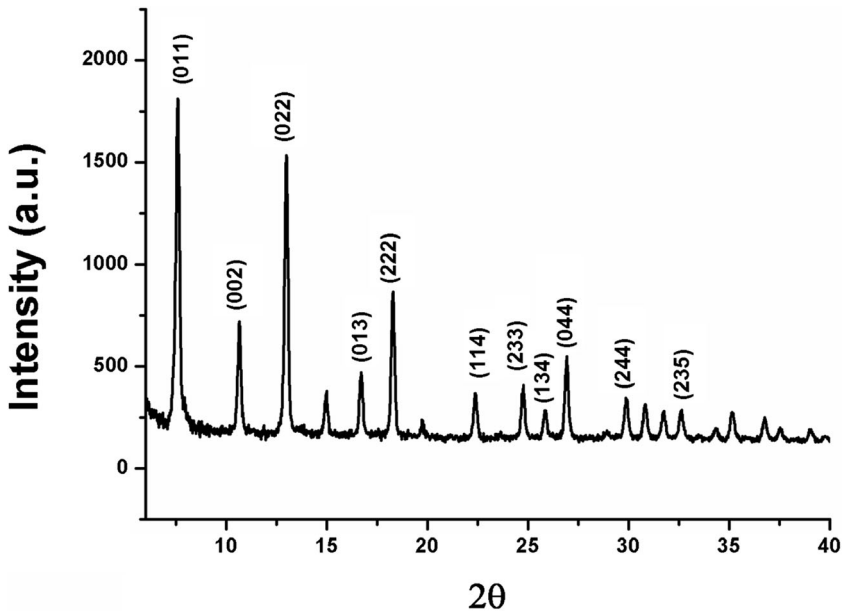

Fig. 1 XRD pattern of ZIF-67

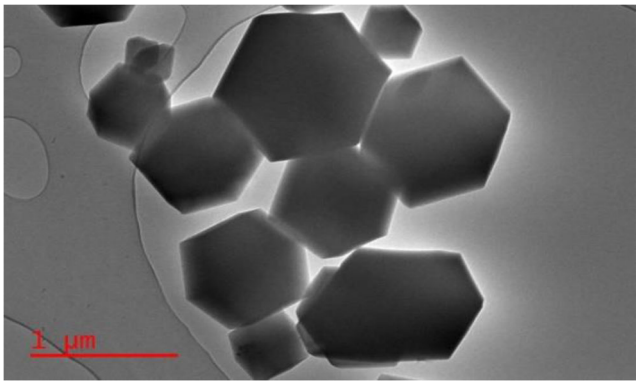

Fig. 2 TEM images of ZIF-67

22.5° (114), 24.7° (233), 25.2° (134), 27.5° (044), 30.1° (244), and 32° (235). These results confirmed that ZIF-67 was successfully synthesized and the results were comparable with previous studies (Gross et al. 2012; Chen 2016 ICCD PDF #15-0806).

Figure 2 shows TEM images of ZIF-67 showing hexagonal shape. Based on previous studies, it has been reported that ZIF-67 shape differs with different molar ratios of metal ion and the ligand and also the time of the synthesis (Yan et al. 2017). At lower molar ratios of the metal to ligand, chamfered cube shapes are observed and at high molar ratios, rhombic-dodecahedral shape of ZIFs are observed (Lin and Chang 2015a, b) and sodalite ZIF can be formed when very small molar ratio is used (1/8), also the metal salt used has an effect on the size of ZIF crystals formed. For example, the use of cobalt nitrate leads to formation of smaller sizes than when cobalt acetate is used (Lin and Chang 2015a, b). In this study, the molar ratio of ¼ which gave results of chamfered-cubic ZIF-67 (also referred to truncated rhombic dodecahedron), was used.

The surface area and pore size distribution of ZIF-67 were found to be 1022 $m^2\ g^{-1}$ and 0.545 $cm^3\ g^{-1}$ respectively with average pore size of 2.13 nm indicates that the material is

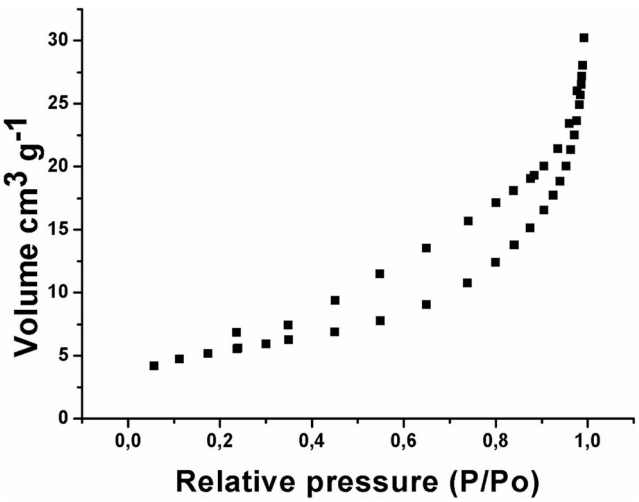

Fig. 3 The nitrogen (N_2) adsorption-desorption isotherms of ZIF-67

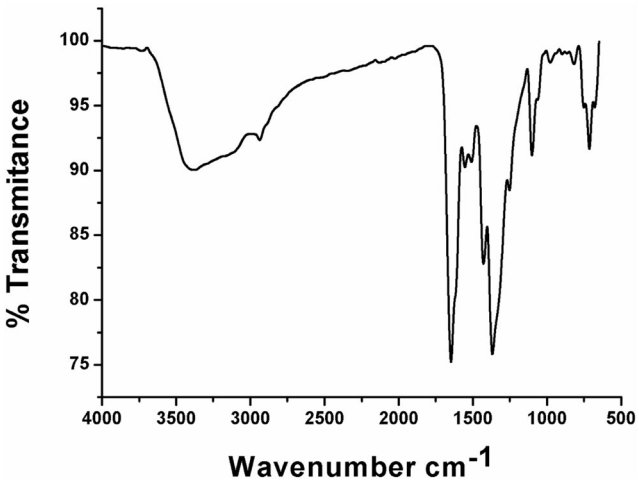

Fig. 4 FTIR spectrum of ZIF-67

mesoporous and the isotherm observed is of type IV. The shape of the N_2 sorption isotherm of ZIF-67 indicates the presence of different pore sizes varying from micropores to mesopores (Fig. 3) (Sun et al. 2016). At low relative pressure area ($P/P_0 < 0.2$), both adsorption and desorption curves displayed an increase which confirms the presence of micropores. There is a slight uptake at high relative pressure closer to 1.0, indicative of macropores (Sun et al. 2016). The large pore size and surface area of ZIF-67 shows that ZIF-67 is the ideal candidate for adsorption of metal ions with high adsorption capacity. The results obtained were comparable to those reported by Sun et al. (2016).

Figure 4 shows FTIR spectrum of ZIF-67 with a broad peak at 3421 cm^{-1} which was ascribed to N–H stretching from the imidazolate ligand. At 1650 cm^{-1}, there is aromatic C=C of the ligand. Another peak was observed around 1430 cm^{-1} which is attributed to C–N of 2-methylimidazole and the peak observed around 550 cm^{-1} corresponds to metal to ligand (Co–N) which confirms the formation of ZIF-67 from cobalt and 2-methylimidazole.

Optimization strategy

To evaluate the effect of influential parameters on the removal of Pb from wastewater, the adsorption experiments were done over a pH range of 3.2–9.7, at different mass of adsorbent (10–30 mg) and contact time (5–34 min). Response surface methodology (RSM) acquired from central composite design (CCD) was used to study the significant factors affecting the adsorption process. The design matrix and percentage removal efficiency as analytical response on three variables/ parameters at five levels are presented in Table S1. Pareto chart reproduced from analysis of variance (ANOVA) was used to evaluate the importance of individual and interactive effects (Fig. 5).

From Pareto chart, the significant effect is represented by the vertical lines, and the bars represent the individual parameters and their interaction. If the bar crosses the confidence

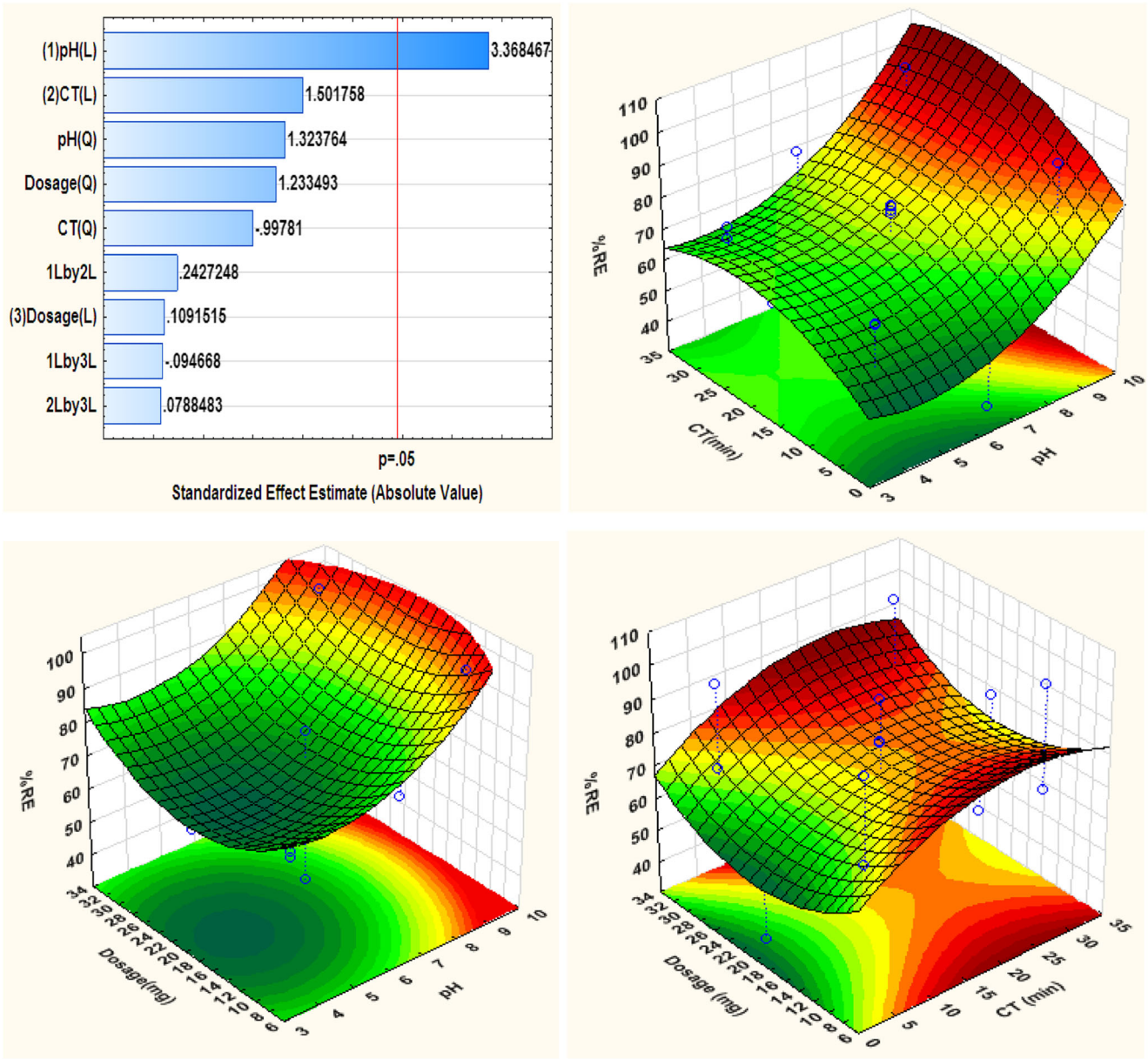

Fig. 5 Pareto chart and 3D response surface plots

line ($p = 0.05$), this indicates that the corresponding interactions or parameters are important at 95% confidence level (Nomngongo and Ngila 2015). It can be seen in Fig. 5 that pH was the most factor for the removal of Pb(II) at 95% confidence level. Other factors (mass of adsorbent and contact time) as well as interactions were insignificant at 95% confidence level. The results obtained suggested that pH of the solution have greater influence in Pb(II) removal.

The relationship between dependent and independent variables were further studied by means of three-dimensional (3D) response surface plots. The 3D response surfaces plots (Fig. 5) were plotted to reveal the interaction of independent variables as well as determining optimal values of each independent variable to obtain maximum response (Mashile et al. 2018).

The response surface plots showed that increase in pH of the synthetic sample leads to increase in removal efficiency. According to literature, the point of zero charge (PZC) for ZIF-67 is 8.7 (Li et al. 2015), this implies that, for values lower than the PZC, the surface of the adsorbent is highly positive. Therefore, at low pH values, the removal efficiency was low owing to the repulsion between Pb(II) and the highly positive surface of the adsorbent. At high pH values, lead exists as cationic form in solution hence the high % removal efficiency was observed. It should be noted that the main driving forces were electrostatic interaction between Pb(II) and ZIF-67, physical adsorption as a result of pores on the surface of the material and coordination bonding. This claim is supported by the results obtained at

Table 2 Adsorption isotherms of Pb(II) on ZIF-67

Isotherms	Parameters	
Langmuir	q_{max} (mg g^{-1})	105
	K_L (L mg^{-1})	15.8
	R^2	0.996
Freundlich	K_F	101
	N	4.48
	R^2	0.959

different pH values as listed in Table S1. It was observed that at lower pH that is below the point of zero charge, the removal efficiency was less than 85% which was due to the physical adsorption and coordination interaction. Above the point of zero charge, the removal efficiency was above 95% due to electrostatic interaction, coordination interaction, and physical adsorption. Figure 5 shows the combined effect of adsorption dosage (mg) and contact time (sonication time in minutes) on the adsorption of Pb(II). It was seen that high surface area of the adsorbent resulted in increased removal percentage with increased adsorbent dosage. Large surface area of ZIF-67 creates more available sites for adsorption with increase in dosage which increases adsorption rate. At lower adsorbent dosage, low percentage removal is observed which is due to inefficiency in reactive sites. According to RSM, the optimized conditions were mass of adsorbent 20 mg, sample pH 9, and contact time 24 min.

Adsorption isotherm models

Equilibrium adsorption data for the removal of Pb(II) was evaluated by Langmuir (Langmuir 1916) and Freundlich (Freundlich 1907). The nonlinear equations for each isotherm model are presented in (Eqns. 3–4):

Langmuir isotherm model

$$q_e = \frac{q_m k_L C_e}{1 + k_L C_e} \tag{3}$$

Where q_{max}: maximum monolayer adsorption capacity (mg g^{-1}), C_e: concentration of adsorbate at equilibrium (mg L^{-1}), and K_L: Langmuir constant (L mg^{-1}).

Freundlich isotherm model

$$q_e = K_F C_e^{\frac{1}{n}} \tag{4}$$

Where q_e: amount of Pb(II) adsorbed (mg/g), C_e: equilibrium concentration of Pb(II) in (mg L^{-1}), K_F is a measure of adsorption capacity and n is an indicator of adsorption effectiveness.

The impact of Pb(II) concentration on the sorbent was investigated in terms of Langmuir and Freundlich models as shown in Figs. S1 and S2. The obtained data from the adsorption of lead fitted the Langmuir isotherm model with higher correlation coefficient R^2 (Table 2). Langmuir model proves that the sorbent is homogeneous which assumes monolayer adsorption as all the sorption sites are uniform. The adsorption capacity reaches a maximum at 40 min with barely increase of adsorption after 40 min.

Table 3 Kinetics of adsorption of Pb(II) on ZIF-67

	Equations	Parameters	Pb
Pseudo-first order	$q_t = q_e[1-\exp(-k_1 t)]$	q_e exp	104
		q_e cal	101
		k_1 (min^{-1})	0.1334
		R^2	0,868
Pseudo-second order	$q_t = \frac{k_2 q_e^2 t}{1 + k_2 q_e t}$	k_2 (g mg^{-1} min^{-1})	0.001615
		q_e (mg g^{-1})	114
		R^2	0,968
Intraparticle diffusion	$q_t = kid\sqrt{t} + C_i$	k_{id1}(mg g^{-1} $min^{1/2}$)	14.1
		C_1 (mg g^{-1})	25.8
		R_1^2	0.983
		k_{id2}(mg g^{-1} $min^{1/2}$)	1.31
		C_2 (mg g^{-1})	93.53
		R_2^2	0.998
Elovich	$q_t = \frac{1}{b}\ln(1 + \alpha B t$	α	73.99
		β	0.0495
		R^2	0.936

q_t: amount of lead adsorbed at time t; q_e: sorption capacity; k_1: rate constant; k_2: second-order constant; C: is the value of intercept which gives information about the boundary layer thickness; k_{id}: intraparticle diffusion rate constant; α is the initial rate constant and β is the desorption constant

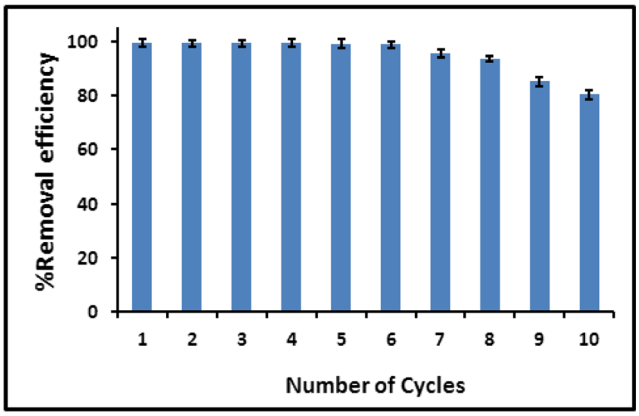

Fig. 6 Regeneration studies

Adsorption kinetics

To understand the rate determining step and mechanism of the adsorption, kinetic were studied using four different kinetics models. The equations and the constants of the models are summarized in Table 3. From Table 3, it can be seen that the data followed the pseudo-second order kinetic model due to its high correlation coefficient greater than 0.968. This suggested that the adsorption process was dominated by chemisorption and to a slighter extent by physisorption (Ghaneian et al. 2017).

Intraparticle diffusion showed that multiple adsorption stages occurred. In addition, the nonlinear plots of intraparticle diffusion did not start from the point of origin and this indicates that boundary layer diffusion was also part of the adsorption of Pb(II) into ZIF-67. Intraparticle diffusion indicated that the adsorptive removal of Pb(II) involved first-boundary layer followed by intraparticle diffusion. The constant C (intercept value that provides an indication of boundary layer thickness) increased from 25.8 to 93.5, with a bigger value for C indicative of bigger effect of boundary layer. This confirms that adsorption of Pb(II) into ZIF-67 was mostly controlled by intraparticle diffusion model. Elovich model was studied to understand the rate determining step. Elovich linear plot showed high correlation efficiency which means intraparticle diffusion was more prominent in Pb(II) sorption by ZIF-67 (Hameed et al. 2008).

Effect of interfering ions

Acid mine drainage contains various ions such as transition metal ions, alkaline earth metals as well as the anions. As a consequence of this, the effect of several and potentially co-existing ions such as Al, Ba, Ca, K, Na, Mg, Cu(II), Co(II), Zn(II), Cd(II), Fe(II), Cr(III), Fe(III), phosphates, chlorides, carbonates, phosphates, and acetates on adsorption of Pb(II) were studied. These ions may contest with the target analyte for the available sites, leading to decrease in its removal from the AMD about 10 mL solution of 2.0 mg L^{-1} lead. The effect of coexisting ions was attained by processing 10 mL solutions 2.0 mg L^{-1} Pb with different metal ions of known concentrations (Table S2–S4). The obtained results indicate that adsorption of Pb(II) onto ZIF-67 was not affected by the presence of other coexisting ion at concentration ranging from 1 to 1000 mg L^{-1}. This is due to the large surface area of ZIF-67, meaning there are more are available sites for the removal of lead. Therefore, the current material (ZIF-67) can adsorb transition metals, anions, and alkaline earth metals.

Desorption and regeneration studies

Regeneration/reusability as well and adsorbent's stability are the most important commercial features in the water treatment process. The regeneration of ZIF-67 was performed by packing the adsorbent in microcolumn. The sample containing 2 mg L^{-1} of Pb (II) was passed through the column at a flow rate of 0.6 mL min^{-1}. ZIF-67 can be regenerated by desorbing the adsorbate (Pb^{2+}) using 0.5 mol L^{-1} of nitric acid. Figure 6 shows that, after eight adsorption/desorption cycles, the adsorption performance of ZIF-67 towards Pb (II) remained the same and the removal efficiency ranged from 99 to 94%. Slight decrease (85–80%) was observed after the eighth cycle. Therefore, it was concluded that ZIF-67 can be recycled at least 8 times without major loss of removal efficiency. This demonstrated that the ZIF-67 had good regeneration and stability for the removal of Pb(II) and can be a candidate for water treatment process.

Table 4 Analysis of real samples

AMD Samples	Concentration of Pb (mg/L) before removal	Concentration of Pb (mg/L) after removal	%Removal efficiency
S1	1.69 ± 0.05	ND	100
S2	3.77 ± 0.12	0.11 ± 0.05	97.1 ± 1.9
S3	2.71 ± 0.06	ND	100
S4	3.43 ± 0.07	0.06 ± 0.01	98.3 ± 1.6
S5	9.77 ± 0.05	2.12 ± 0.12	78.3 ± 2.1

ND, not detected

Table 5 Comparison of amount of lead adsorbed by different adsorbents

Adsorbent	Adsorption capacity (mg/g)	References
MCNB	2.86	Luo et al. 2016
Fe_3O_4	53	Rajput et al. 2016
MIL 101	120	Salarian et al. 2014
ED-MIL-101	81.09	Luo et al. 2015
Chitin	60.24	Siahkamari et al. 2017
Acidic cation resin	64	Vergili et al. 2013
Zeolite-supported nanoscale zero-valent iron	85.90	Li et al. 2018
Commercial activated carbon	47.2	Largitte et al. 2014
ZIF-67	105	Current work

Application to real samples

The practical applicability of ZIF 67 was evaluated by performing adsorption of lead from acid mine drainage samples. The AMD was first filtered to remove particulates and analyzed using optimized procedure to get the percentage removal efficiency. From Table 4, the removal efficiencies for Pb^{2+} ranged from 78.3–100%. These results demonstrated that ZIF-67 can be used for adsorption of lead ions in real complex such as AMD sample with relatively high removal efficiency.

Various materials that were previously used in Pb(II) removal from different water matrices, some of the materials are presented in Table 5 with adsorption capacities. As seen in Table 5, ZIF-67 is better or comparable with other materials.

Conclusion

It was observed that ZIF-67 was the best candidate for removal of lead from AMD. Two adsorption isotherms, i.e., Langmuir and Freundlich, were studied; the obtained equilibrium data best fitted Langmuir model. The maximum adsorption capacity of 105 mg g^{-1} was obtained. The best fit in kinetic studies was obtained when using pseudo-second-order kinetic model revealing chemical adsorption characteristics of Pb(II) on ZIF-67. In addition, Elovich model showed that diffusion rate determining step is more prominent in Pb(II) sorption by ZIF-67. The study demonstrated that coexisting ions found in AMD samples used had no detrimental influence on the removal of Pb ions. Therefore, the current material (ZIF-67) can adsorb transition metals, anions, and alkaline earth metals. After dilute nitric acid treatment, the ZIF-67 adsorbent showed good stability and could be regenerated and reused up to 8 cycles.

Funding information The authors gratefully acknowledge the National Research Foundation (NRF) Innovation (Grant no. 113014) and DST/Mintek Nanotechnology Innovation Centre (NIC) for financial support. They are thankful to the Department of Applied Chemistry Faculty of Science University of Johannesburg.

Compliance with ethical standards

Conflict of interest The authors declare that they have no conflict of interest.

References

Aldawsari A, Khan MA, Hameed BH, Alqadami AA, Siddiqui MR, Alothman ZA, Ahmed AYBH (2017) Mercerized mesoporous date pit activated carbon—a novel adsorbent to sequester potentially toxic divalent heavy metals from water. PLoS One 12(9):e0184493

Al-Qodah Z, Yahya MA, Al-Shannag M (2017) On the performance of bioadsorption processes for heavy metal ions removal by low-cost agricultural and natural by-products bioadsorbent: a review. Desalin Water Treat 85:339–357

Amini M, Younesi H, Bahramifar N, Lorestani AAZ, Ghorbani F, Daneshi A, Sharifzadeh M (2008) Application of response surface methodology for optimization of lead biosorption in an aqueous solution by *Aspergillus niger*. J Hazard Mater 154(1–3):694–702

An HJ, Bhadra BN, Khan NA, Jhung SH (2018) Adsorptive removal of wide range of pharmaceutical and personal care products from water by using metal azolate framework-6-derived porous carbon. Chem Eng J 343:447–454

Bo S, Ren W, Lei C, Xie Y, Cai Y, Wang S, Gao J, Ni Q, Yao J (2018) Flexible and porous cellulose aerogels/zeolitic imidazolate framework (ZIF-8) hybrids for adsorption removal of Cr (IV) from water. J Solid State Chem 262:135–141

Chen B (2016) Zeolitic imidazolate frameworks (ZIFs) and their derivatives: synthesis and energy related applications

Dey T (2012) Nanotechnology for water purification. Universal-Publishers, Irvine

Dimpe KM, Ngila JC, Nomngongo PN (2017) Application of waste tyre-based activated carbon for the removal of heavy metals in wastewater. Cogent Eng 4(1):1330912

Fernandez-Rojo L, Héry M, Le Pape P, Braungardt C, Desoeuvre A, Torres E, Tardy V, Resongles E, Laroche E, Delpoux S, Joulian C (2017) Biological attenuation of arsenic and iron in a continuous

flow bioreactor treating acid mine drainage (AMD). Water Res 123: 594–606

Freundlich H (1907) Über die adsorption in lösungen. Z. Phys. Chem. (N F) 57(1):385–470

Ghaneian MT, Bhatnagar A, Ehrampoush MH, Amrollahi M, Jamshidi B, Dehvari M, Taghavi M (2017) Biosorption of hexavalent chromium from aqueous solution onto pomegranate seeds: kinetic modeling studies. Int J Environ Sci Technol 14(2):331–340

Gomar M, Yeganegi S (2018) Corrigendum to "Adsorption of 5-fluorouracil, hydroxyurea and mercaptopurine drugs on zeolitic imidazolate frameworks (ZIF-7, ZIF-8 and ZIF-9)". Microporous Mesoporous Mater 258:277–280

Gross AF, Sherman E, Vajo JJ (2012) Aqueous room temperature synthesis of cobalt and zinc sodalite zeolitic imidizolate frameworks. Dalton Trans 41(18):5458–5460

Hameed BH, Tan IAW, Ahmad AL (2008) Adsorption isotherm, kinetic modeling and mechanism of 2, 4, 6-trichlorophenol on coconut husk-based activated carbon. Chem Eng J 144(2):235–244

Han TT, Bai HL, Liu YY, Ma JF (2018) Synthesis of nanoporous cobalt/carbon materials by a carbonized zeolitic imidazolate framework-9 and adsorption of dyes. New J Chem 42(1):717–724

Huang YB, Liang J, Wang XS, Cao R (2017) Multifunctional metal–organic framework catalysts: synergistic catalysis and tandem reactions. Chem Soc Rev 46(1):126–157

Huang L, He M, Chen B, Hu B (2018a) Magnetic Zr-MOFs nanocomposites for rapid removal of heavy metal ions and dyes from water. Chemosphere 199:435–444

Huang Y, Zeng X, Guo L, Lan J, Zhang L, Cao D (2018b) Heavy metal ion removal of wastewater by zeolite-imidazolate frameworks. Sep Purif Technol 194:462–469

Huo JB, Xu L, Yang JCE, Cui HJ, Yuan B, Fu ML (2018) Magnetic responsive Fe 3 O 4-ZIF-8 core-shell composites for efficient removal of As (III) from water. Colloids Surf A Physicochem Eng Asp 539:59–68

Jin WG, Chen W, Xu PH, Lin XW, Huang XC, Chen GH, Lu F, Chen XM (2017) An exceptionally water stable metal-organic framework with amide-functionalized cages: selective CO_2/CH_4 uptake, removal of antibiotics and dyes from water. Chemistry 23(53):13058–13066

Jung BK, Jun JW, Hasan Z, Jhung SH (2015) Adsorptive removal of p-arsanilic acid from water using mesoporous zeolitic imidazolate framework-8. Chem Eng J 267:9–15

Kang Z, Wang S, Fan L, Xiao Z, Wang R, Sun D (2017) Surface wettability switching of metal-organic framework mesh for oil-water separation. Mater Lett 189:82–85

Kummu M, Guillaume JHA, De Moel H, Eisner S, Flörke M, Porkka M, Siebert S, Veldkamp TIE, Ward PJ (2016) The world's road to water scarcity: shortage and stress in the 20th century and pathways towards sustainability. Sci Rep 6:38495

Langmuir I (1916) The constitution and fundamental properties of solids and liquids. Part I. Solids. J Am Chem Soc 38(11):2221–2295

Largitte L, Gervelas S, Tant T, Dumesnil PC, Hightower A, Yasami R, Bercion Y, Lodewyckx P (2014) Removal of lead from aqueous solutions by adsorption with surface precipitation. Adsorption 20(5–6):689–700

Le Pape P, Battaglia-Brunet F, Parmentier M, Joulian C, Gassaud C, Fernandez-Rojo L, Guigner JM, Ikogou M, Stetten L, Olivi L, Casiot C (2017) Complete removal of arsenic and zinc from a heavily contaminated acid mine drainage via an indigenous SRB consortium. J Hazard Mater 321:764–772

Lee H, Kim D, Kim J, Ji MK, Han YS, Park YT, Yun HS, Choi J (2015) As (III) and As (V) removal from the aqueous phase via adsorption onto acid mine drainage sludge (AMDS) alginate beads and goethite alginate beads. J Hazard Mater 292:146–154

Li X, Gao X, Ai L, Jiang J (2015) Mechanistic insight into the interaction and adsorption of Cr (VI) with zeolitic imidazolate framework-67 microcrystals from aqueous solution. Chem Eng J 274:238–246

Li Z, Huang X, Sun C, Chen X, Hu J, Stein A, Tang B (2017) Thin-film electrode based on zeolitic imidazolate frameworks (ZIF-8 and ZIF-67) with ultra-stable performance as a lithium-ion battery anode. J Mater Sci 52(7):3979–3991

Li Z, Wang L, Meng J, Liu X, Xu J, Wang F, Brookes P (2018) Zeolite-supported nanoscale zero-valent iron: new findings on simultaneous adsorption of Cd (II), Pb (II), and As (III) in aqueous solution and soil. J Hazard Mater 344:1–11

Lin KYA, Chang HA (2015a) Ultra-high adsorption capacity of zeolitic imidazole framework-67 (ZIF-67) for removal of malachite green from water. Chemosphere 139:624–631

Lin KYA, Chang HA (2015b) Zeolitic imidazole framework-67 (ZIF-67) as a heterogeneous catalyst to activate peroxymonosulfate for degradation of rhodamine B in water. J Taiwan Inst Chem Eng 53:40–45

Luo X, Ding L, Luo J (2015) Adsorptive removal of Pb (II) ions from aqueous samples with amino-functionalization of metal–organic frameworks MIL-101 (Cr). J Chem Eng Data 60(6):1732–1743

Luo X, Lei X, Xie X, Yu B, Cai N, Yu F (2016) Adsorptive removal of lead from water by the effective and reusable magnetic cellulose nanocomposite beads entrapping activated bentonite. Carbohydr Polym 151:640–648

Maarof HI, Daud WMAW, Aroua MK (2017) Recent trends in removal and recovery of heavy metals from wastewater by electrochemical technologies. Rev Chem Eng 33(4):359–386

Marzougui, Z., Damak, M., Elleuch, B., Elaissari, A., 2017. Occurrence and enhanced removal of heavy metals in industrial wastewater treatment plant using coagulation-flocculation process. In Euro-Mediterranean conference for environmental Integration 535–538

Mashile PP, Mpupa A, Nomngongo PN (2018) Adsorptive removal of microcystin-LR from surface and wastewater using tyre-based powdered activated carbon: kinetics and isotherms. Toxicon 145:25–31

Mohajeri S, Aziz HA, Isa MH, Zahed MA, Adlan MN (2010) Statistical optimization of process parameters for landfill leachate treatment using electro-Fenton technique. J Hazard Mater 176(1–3):749–758

Nayak A, Bhushan B, Gupta V, Sharma P (2017) Chemically activated carbon from lignocellulosic wastes for heavy metal wastewater remediation: effect of activation conditions. J Colloid Interface Sci 493:228–240

Nomngongo PN, Ngila JC (2015) Multivariate optimization of dual-bed solid phase extraction for preconcentration of Ag, Al, As and Cr in gasoline prior to inductively coupled plasma optical emission spectrometric determination. Fuel 139:285–291

Panchariya DK, Rai RK, Anil Kumar E, Singh SK (2018) Core–shell zeolitic imidazolate frameworks for enhanced hydrogen storage. ACS Omega 3(1):167–175

Perrich JR (2018) Activated carbon adsorption for wastewater treatment. CRC Press, Boca Raton

Premkumar MP, Thiruvengadaravi KV, Kumar PS, Nandagopal J, Sivanesan S (2018) Eco-friendly treatment strategies for wastewater containing dyes and heavy metals. In: Gupta T, Agarwal A, Agarwal R, Labhsetwar N (eds) Environmental contaminants. Energy, environment, and sustainability. Springer, Singapore, pp 317–360

Rajput S, Pittman CU Jr, Mohan D (2016) Magnetic magnetite (Fe3O4) nanoparticle synthesis and applications for lead (Pb^{2+}) and chromium (Cr^{6+}) removal from water. J Colloid Interface Sci 468:334–346

Sadegh H, Ali GA, Gupta VK, Makhlouf ASH, Shahryari-ghoshekandi R, Nadagouda MN, Sillanpää M, Megiel E (2017) The role of nanomaterials as effective adsorbents and their applications in wastewater treatment. J Nanostruct Chem 7(1):1–14

Saeed MO, Azizli K, Isa MH, Bashir MJ (2015) Application of CCD in RSM to obtain optimize treatment of POME using Fenton oxidation process. J Water Process Eng 8:7–16

Sahin O, Stewart RA, Porter MG (2015) Water security through scarcity pricing and reverse osmosis: a system dynamics approach. J Clean Prod 88:160–171

Salarian M, Ghanbarpour A, Behbahani M, Bagheri S, Bagheri A (2014) A metal-organic framework sustained by a nanosized Ag12 cuboctahedral node for solid-phase extraction of ultratraces of lead (II) ions. Microchim Acta 181(9–10):999–1007

Samal M, Panda J, Biswal BP, Sahu R (2018) Kitchen grinder: a tool for the synthesis of metal-organic framework towards size selective dye adsorption. Cryst Eng Comm 20(18):2486–2490

Santhosh C, Daneshvar E, Kollu P, Peräniemi S, Grace AN, Bhatnagar A (2017) Magnetic SiO2@ CoFe2O4 nanoparticles decorated on graphene oxide as efficient adsorbents for the removal of anionic pollutants from water. Chem Eng J 322:472–487

Shahrak MN, Ghahramaninezhad M, Eydifarash M (2017) Zeolitic imidazolate framework-8 for efficient adsorption and removal of Cr (VI) ions from aqueous solution. Environ Sci Pollut Res Int 24(10):9624–9634

Siahkamari M, Jamali A, Sabzevari A, Shakeri A (2017) Removal of Lead (II) ions from aqueous solutions using biocompatible polymeric nano-adsorbents: a comparative study. Carbohydr Polym 157: 1180–1189

Sun W, Zhai X, Zhao L (2016) Synthesis of ZIF-8 and ZIF-67 nanocrystals with well-controllable size distribution through reverse microemulsions. Chem Eng J 289:59–64

Ungureanu G, Santos S, Boaventura R, Botelho C (2015) Arsenic and antimony in water and wastewater: overview of removal techniques with special reference to latest advances in adsorption. J Environ Manag 151:326–342

Vergili I, Soltobaeva G, Kaya Y, Gonder ZB, Çavuş S, Gurdag S (2013) Study of the removal of Pb(II) using a weak acidic cation resin: kinetics, thermodynamics, equilibrium, and breakthrough curves. Ind Eng Chem Res 52:9227–9238

Wu X, Liu W, Wu H, Zong X, Yang L, Wu Y, Ren Y, Shi C, Wang S, Jiang Z (2018) Nanoporous ZIF-67 embedded polymers of intrinsic microporosity membranes with enhanced gas separation performance. J Membr Sci 548:309–318

Xu M, McKay G (2017) Removal of heavy metals, lead, cadmium, and zinc, using adsorption processes by cost-effective adsorbents. In Adsorption processes for water treatment and purification Cham: Springer. (pp. 109–138)

Yadav DK, Srivastava S (2017) Carbon nanotubes as adsorbent to remove heavy metal ion (Mn^{+7}) in wastewater treatment. Mater Today: Proc 4(2):4089–4094

Yan X, Hu X, Chen T, Zhang S, Zhou M (2017) Adsorptive removal of 1-naphthol from water with zeolitic imidazolate framework-67. J Phys Chem Solids 107:50–54

Yurekli Y (2016) Removal of heavy metals in wastewater by using zeolite nano-particles impregnated polysulfone membranes. J Hazard Mater 309:53–64

Zanin E, Scapinello J, de Oliveira M, Rambo CL, Franscescon F, Freitas L, de Mello JMM, Fiori MA, Oliveira JV, Dal Magro J (2017) Adsorption of heavy metals from wastewater graphic industry using clinoptilolite zeolite as adsorbent. Process Saf Environ Prot 105: 194–200

Zhang W, Tan Y, Gao Y, Wu J, Hu J, Stein A, Tang B (2016) Nanocomposites of zeolitic imidazolate frameworks on graphene oxide for pseudocapacitor applications. J Appl Electrochem 46(4): 441–450

Zhang S, Yang Q, Yang X, Wang W, Li Z, Zhang L, Wang C, Wang Z (2017) A zeolitic imidazolate framework based nanoporous carbon as a novel fiber coating for solid-phase microextraction of pyrethroid pesticides. Talanta 166:46–53